Instabilities and Pattern Formation in Active Particle Suspensions: Kinetic Theory and Continuum Simulations

David Saintillan* and Michael J. Shelley

Courant Institute of Mathematical Sciences, New York University, New York, New York 10012, USA

(Received 3 October 2007; published 29 April 2008)

We use kinetic theory and nonlinear continuum simulations to study the collective dynamics in suspensions of self-propelled particles. The stability of aligned suspensions is first analyzed, and we demonstrate that such suspensions are always unstable to fluctuations, a result that generalizes previous predictions by Simha and Ramaswamy. Isotropic suspensions are also considered, and it is shown that an instability for the particle stress occurs in that case. Using simulations, nonlinear effects are investigated, and the long-time behavior of the suspensions is observed to be characterized by the formation of strong density fluctuations, resulting in efficient fluid mixing.

DOI: 10.1103/PhysRevLett.100.178103 PACS numbers: 87.18.Ed, 87.10.−e, 87.18.Hf

A suspension of self-propelled particles, an example of an *active suspension*, can exhibit complex dynamics as a result of long-ranged hydrodynamic interactions. Such suspensions occur commonly in nature, where microorganisms develop in large-scale colonies [1], as well as in technological applications where artificial [2–4] or biological swimmers may be used to achieve various tasks, such as enhancing fluid mixing [5]. Previous studies on dilute suspensions in thin films have indeed shown strong hydrodynamic diffusion [6]. In concentrated bulk suspensions, large-scale spatially and temporally correlated motions as well as concentration patterns have been observed and characterized experimentally by Dombrowski *et al.* [7] and Tuval *et al.* [8] (see also [9–12]). On the basis of an analogy with sedimentation, they conjectured that the large-scale dynamics resulted from hydrodynamic coupling. These studies suggest that a homogeneous distribution is not a stable configuration, and that an active suspension will spontaneously evolve towards a nontrivial dynamical state. Identifying mechanisms leading to this pattern formation is the goal of this Letter.

Hydrodynamic interactions among self-propelled particles have also been studied in numerical models, with various levels of approximation [13–15]. These simulations have captured salient features of experiments, including hydrodynamic diffusion, large-scale collective motions and strong density fluctuations. Particle simulations are however limited in size owing to their high computational cost. As an alternative, kinetic theories have long been used to study suspensions of long-chain and rodlike molecules [16]. These can, in principle, be adapted to suspensions of self-propelled particles by appropriate modifications of particle fluxes and induced extra stress. A linear, long-wave version of such a model was proposed by Simha and Ramaswamy [17]. Here, a more general kinetic model is derived to study dynamics in active suspensions. It is first shown that aligned suspensions of self-propelled particles are always unstable to fluctuations, a result that generalizes the prediction of Ref. [17]. We also consider initially isotropic suspensions and find that an instability for the particle stress also takes place in that case for *pushers*—tail-actuated swimmers—but not for *pullers*. Finally, we use nonlinear simulations to study the long-time behavior in these systems.

While different types of swimmers use different propulsion mechanisms, universal features exist in the induced hydrodynamics. In particular, a particle exerts a propulsive force $\mathbf{F}_p$ on the surrounding fluid (which may be the resultant of the beating of cilia or flagella), which is balanced by the resistive drag $\mathbf{F}_d = -\mathbf{F}_p$ due to the surrounding fluid. To leading order, the forcing exerted by the particle on the fluid is therefore a force dipole, the strength of which we denote by σ_0. This dipole forcing creates a disturbance flow, the characteristics of which are universal in the far-field for many types of self-propelled particles. This general feature is the basis of the present model.

The evolution of a suspension of rodlike particles is described by a continuity equation for the distribution function $\Psi(\mathbf{x}, \mathbf{p}, t)$ of the particle center-of-mass position $\mathbf{x}$ and director $\mathbf{p}$ [16]:

$$\partial_t \Psi = -\nabla_{\mathbf{x}} \cdot (\dot{\mathbf{x}}\Psi) - \nabla_{\mathbf{p}} \cdot (\dot{\mathbf{p}}\Psi). \tag{1}$$

The distribution function is normalized as follows: $\frac{1}{V} \times \int_V d\mathbf{x} \int d\mathbf{p} \Psi(\mathbf{x}, \mathbf{p}, t) = n$, where V is volume of the region of interest, and n is the mean number density in the suspension.

The continuity Eq. (1) involves flux velocities in $\mathbf{x}$ and $\mathbf{p}$, which for rodlike particles swimming in the direction of $\mathbf{p}$ can be modeled as

$$\dot{\mathbf{x}} = U_0\mathbf{p} + \mathbf{u} - D\nabla_{\mathbf{x}}(\ln\Psi), \tag{2}$$

$$\dot{\mathbf{p}} = (\mathbf{I} - \mathbf{pp}) \cdot [(\gamma\mathbf{E} + \mathbf{W}) \cdot \mathbf{p} - d_r\nabla_{\mathbf{p}}(\ln\Psi)]. \tag{3}$$

In Eq. (2), the center-of-mass velocity of a particle is represented as the sum of its swimming velocity $U_0\mathbf{p}$ and of the local fluid velocity $\mathbf{u}(\mathbf{x}, t)$ induced by the particles in

the suspension. Similarly, the orientational velocity in Eq. (3) arises from the fluid velocity and is modeled using Jeffery's equation [18] in terms of the fluid rate-of-strain and vorticity tensors: $\mathbf{E} = (\nabla\mathbf{u} + \nabla\mathbf{u}^T)/2$, $\mathbf{W} = (\nabla\mathbf{u} - \nabla\mathbf{u}^T)/2$, and a shape parameter $-1 \le \gamma \le 1$, with $\gamma \approx 1$ for rods. Both center-of-mass and rotary diffusion can be accounted for through the diffusivities D and d_r, which may model the effects of hydrodynamic dispersion or particle tumbling, and are assumed constants in this work.

To close the equations, the velocity $\mathbf{u}(\mathbf{x}, t)$ of the fluid is determined through the Stokes equations:

$$-\eta\nabla_{\mathbf{x}}^2\mathbf{u} + \nabla_{\mathbf{x}}q = \nabla_{\mathbf{x}} \cdot \boldsymbol{\Sigma}^p, \qquad \nabla_{\mathbf{x}} \cdot \mathbf{u} = 0, \quad (4)$$

where η denotes the fluid viscosity and q is the pressure. Neglecting higher-order terms from particle interactions, the fluid motion arises from the active particle stress $\boldsymbol{\Sigma}^p(\mathbf{x}, t)$ defined as

$$\boldsymbol{\Sigma}^p(\mathbf{x}, t) = \sigma_0 \int \Psi(\mathbf{x}, \mathbf{p}, t)\left(\mathbf{pp} - \frac{\mathbf{I}}{3}\right)d\mathbf{p}. \quad (5)$$

$\boldsymbol{\Sigma}^p$ can be viewed as a configuration average over all orientations $\mathbf{p}$ of the force dipoles $\sigma_0(\mathbf{pp} - \mathbf{I}/3)$ exerted by the particles on the fluid [19]; it may also be interpreted as a nematic order parameter weighted by the local concentration. The stress magnitude σ_0 can be shown to be related to the swimming velocity U_0 by $\sigma_0/\eta U_0 l^2 = \alpha$ [14,17], where l is the characteristic dimension of the particles and α is a dimensionless $O(1)$ constant that depends on the swimming mechanism. A particle that propels itself by exerting a force near its tail (*pusher*) will result in $\sigma_0 < 0$ (and $\alpha < 0$), whereas a particle that propels itself using its head (*puller*) will result in $\sigma_0 > 0$ ($\alpha > 0$) [17]. In the following, we consider both cases but focus specifically on the case of pushers ($\sigma_0 < 0$), which presents more interesting dynamical features.

All the equations can be made dimensionless using the following velocity, length, and time scales: $u_c = U_0$, $l_c = (nl^2)^{-1}$, $t_c = l_c/u_c$; in addition, the distribution function is scaled by n. After nondimensionalization, the only parameters remaining in the equations are the dimensionless stress magnitude α, the shape parameter γ, and the dimensionless diffusivities D and d_r. The only dependence on the number density n then occurs through the system size, which is made dimensionless by $(nl^2)^{-1}$.

Linear instabilities.—We first analyze the linear stability of a nearly aligned suspension in the case where diffusion can be neglected ($D \equiv 0$, $d_r \equiv 0$). If a single particle director exists at a given location $\mathbf{x}$, i.e., for $\Psi(\mathbf{x}, \mathbf{p}, t) = c(\mathbf{x}, t)\delta[\mathbf{p} - \mathbf{n}(\mathbf{x}, t)]$, and if diffusion is negligible, the continuity Eq. (1) can be replaced by two evolution equations for the local concentration field $c(\mathbf{x}, t)$ and director field $\mathbf{n}(\mathbf{x}, t)$ [20]:

$$\partial_t c + \nabla_{\mathbf{x}} \cdot [(\mathbf{n} + \mathbf{u})c] = 0, \quad (6)$$

$$\partial_t \mathbf{n} + (\mathbf{n} + \mathbf{u}) \cdot \nabla_{\mathbf{x}}\mathbf{n} = (\mathbf{I} - \mathbf{nn}) \cdot (\gamma\mathbf{E} + \mathbf{W}) \cdot \mathbf{n}. \quad (7)$$

In that case, the velocity field $\mathbf{u}(\mathbf{x}, t)$ still satisfies the Stokes Eqs. (4), with the simplified active stress tensor: $\boldsymbol{\Sigma}^p(\mathbf{x}, t) = \alpha c(\mathbf{x}, t)(\mathbf{nn} - \mathbf{I}/3)$.

We consider a nearly uniform suspension in which the particles are all nearly aligned along the $\hat{\mathbf{z}}$ direction: $c(\mathbf{x}, t) = 1 + \epsilon c'(\mathbf{x}, t)$, $\mathbf{n}(\mathbf{x}, t) = \hat{\mathbf{z}} + \epsilon\mathbf{n}'(\mathbf{x}, t)$, where $\mathbf{n}' \cdot \hat{\mathbf{z}} = 0$ and $|\epsilon| \ll 1$. Specifically, we seek plane-wave solutions with wave vector $\mathbf{k}$: $c'(\mathbf{x}, t) = \tilde{c}(\mathbf{k}) \exp i(\mathbf{k} \cdot \mathbf{x} - \omega t)$ with a similar expression for $\mathbf{n}'$. Substitution into Eqs. (6) and (7) and linearization to $O(\epsilon)$ gives an eigenvalue problem for $\omega_\pm(k) = k\cos\theta + i\lambda_\pm(k)$, and yields

$$\lambda_\pm = \frac{1}{2}f(\theta)\cos 2\theta\left[1 \pm \left(1 + 4ik\frac{\sin^2\theta\cos\theta}{f(\theta)\cos^2 2\theta}\right)^{1/2}\right]. \quad (8)$$

We have defined $k = |\mathbf{k}|$, $\hat{\mathbf{k}} \cdot \hat{\mathbf{z}} = \cos\theta$, and $f(\theta) = -\alpha[(\gamma + 1)\cos^2\theta - (\gamma - 1)\sin^2\theta]/2$.

The growth-rate $\omega_i = \mathrm{Re}(\lambda_\pm)$ is plotted vs k and θ in Fig. 1 for $\alpha = -1$, $\gamma = 1$ (the case $\alpha = 1$ is obtained by changing the sign of ω_i). It can be shown that for $k > 0$ the two growth rates have opposite signs. In particular, there is always a positive growth rate; i.e., suspensions of aligned particles are always unstable to density and orientation perturbations. In the long-wave limit ($k \to 0$), the two eigenvalues become $\omega_+ = f(\theta)\cos 2\theta$ and $\omega_- = 0$. The nonzero eigenvalue is that previously obtained in Ref. [17], where it was concluded that only certain ranges of wave angles were subject to an instability. Because it includes finite wave number contributions, our theory picks up the additional eigenvalue ω_- in addition to that found by Simha and Ramaswamy [21]. This is consistent with our previous particle simulations [14], which showed an instability for all wave angles. At high wave numbers, the present theory predicts an increase in growth-rate with k: in a real system, however, one should expect diffusion to stabilize high-wave-number fluctuations.

The stability of isotropic suspensions, which may be more relevant to biological systems, can also be considered based on the general continuity Eq. (1), by decomposing the distribution function as

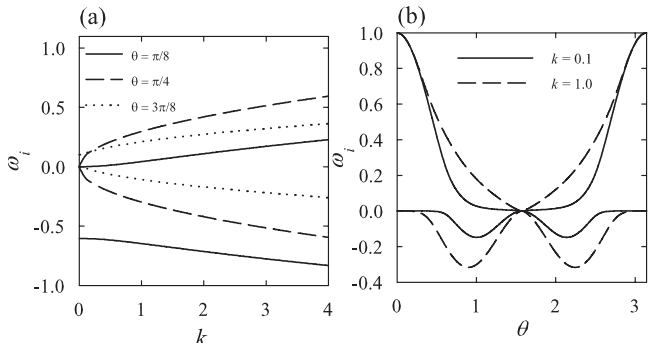

FIG. 1. Growth rates $\omega_i = \mathrm{Re}(\lambda_\pm)$ in a suspension of nearly aligned swimming particles as function of (a) the wave vector k for various wave angles, and (b) the wave angle θ for $k = 0.1$ and $k = 1.0$, obtained from Eq. (8).

$$\Psi(\mathbf{x}, \mathbf{p}, t) = [1 + \epsilon\Psi'(\mathbf{x}, \mathbf{p}, t)]/4\pi, \quad (9)$$

with $|\epsilon| \ll 1$. For ease of analysis, we neglect angular diffusion ($d_r \equiv 0$), but do account for center-of-mass diffusion. Again, we consider a plane-wave perturbation for the distribution function: $\Psi'(\mathbf{x}, \mathbf{p}, t) = \tilde{\Psi}(\mathbf{p}, \mathbf{k}) \times \exp i(\mathbf{k} \cdot \mathbf{x} - \omega t)$ (note that this system is non-normal). Substituting (9) into the Stokes Eqs. (4) and into the continuity Eq. (1) and linearizing the equations to $O(\epsilon)$, it can be shown that the stability problem reduces to an eigenvalue problem for the perturbation active particle stress tensor $\tilde{\boldsymbol{\Sigma}}^p$, written formally as [20] $\tilde{\boldsymbol{\Sigma}}^p = \alpha\gamma\boldsymbol{\Pi}(\mathbf{k}, \omega):\tilde{\boldsymbol{\Sigma}}^p$, where the operator $\boldsymbol{\Pi}(\mathbf{k}, \omega)$ is a fourth-order tensor. In particular, it can be shown that the eigenmodes leading to an instability are active shear stresses of the form $\tilde{\boldsymbol{\Sigma}}^p = \hat{\mathbf{k}}\hat{\mathbf{k}}_\perp + \hat{\mathbf{k}}_\perp\hat{\mathbf{k}}$, where $\hat{\mathbf{k}}_\perp$ is any unit vector perpendicular to $\hat{\mathbf{k}}$. The dispersion relation for these modes is given by [20]

$$\frac{3i\alpha\gamma}{2k}\left[2a^3 - \frac{4}{3}a + (a^4 - a^2)\log\left(\frac{a-1}{a+1}\right)\right] = 1, \quad (10)$$

where $a = -(\omega + iDk^2)/k$.

Equation (10) was solved numerically for $\omega(k)$. The solution for $\alpha = -1$, $\gamma = 1$ and $D = 0$ is shown in Fig. 2 where the real and imaginary parts of ω are plotted vs k. We observe that at low values of k, $\omega_r \equiv 0$ and $\omega_i > 0$; i.e., low-wave-number shear stress fluctuations will amplify exponentially in suspensions of pushers. At higher wave numbers ($k \gtrsim 0.34$), ω_r becomes positive; i.e., stress oscillations will occur and amplify. At yet higher wave numbers, ω_i becomes zero and stress fluctuations are stable: in the absence of diffusion we therefore can expect the instability to occur at all length scales $\gtrsim (nl^2)^{-1}$. Including center-of-mass diffusion ($D > 0$) simply shifts the solution for ω_i by $-Dk^2$, which results in a more rapid damping of the instability at high wave numbers; low wave numbers, however, always remain unstable. In the case of pullers ($\alpha > 0$), the sign of ω_i changes in Fig. 2(b), which suggests that long-wave density fluctuations do not grow in that case.

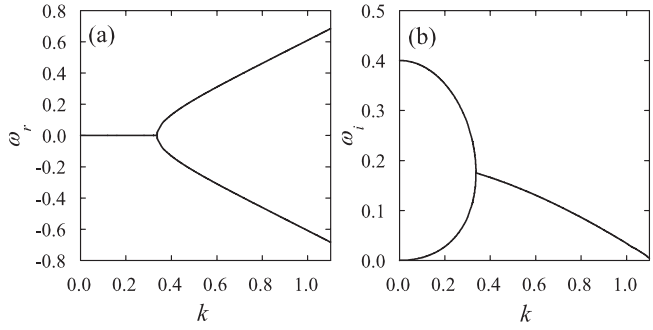

FIG. 2. (a) Real part ω_r and (b) imaginary part ω_i of the complex frequency ω as a function of k in a nearly isotropic suspension, in the case $\alpha = -1$, $\gamma = 1$ and $D = 0$, obtained by numerically solving the dispersion relation (10).

Nonlinear dynamics.—To study the long-time dynamics and pattern formation of the instabilities, nonlinear numerical simulations were performed by integrating Eq. (1) in two dimensions, with both center-of-mass and rotary diffusion. The results shown here are for pushers ($\alpha = -1$, $\gamma = 1$); simulations for pullers ($\alpha > 0$) were also performed but did not show any instability (in agreement with the linear stability result) and are therefore not shown here. An initial condition of the form (9) was used, in which the initial perturbation Ψ' is a band-limited sum of random Fourier modes. Figure 3 shows maps of the concentration field c and mean director field $\mathbf{n}$ at various times, where c and $\mathbf{n}$ are defined as $c(\mathbf{x}, t) = \int \Psi d\mathbf{p}$ and $\mathbf{n}(\mathbf{x}, t) = (\int \mathbf{p}\Psi d\mathbf{p})/c(\mathbf{x}, t)$. Note that c and $\mathbf{n}$ satisfy $\partial_t c + \mathbf{u} \cdot \nabla c = -\nabla \cdot (c\mathbf{n})$. At $t = 0$, the imposed distribution contains fluctuations at many length scales, and the mean director field $\mathbf{n}$ only exhibits correlation over very short scales. As the instability develops ($t = 60$), short-scale fluctuations disappear, leading to a smooth director field with correlated orientations over the size of the box: this is a consequence of the active stress instability, since the active stress tensor can be viewed as a nematic order

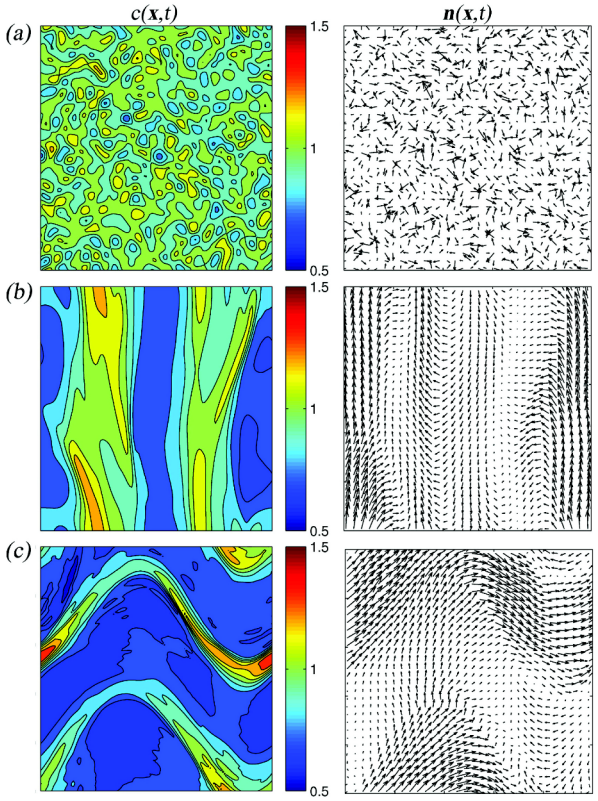

FIG. 3 (color online). Snapshots of the local concentration c and mean director field $\mathbf{n}$ at various times: (a) $t = 0.0$, (b) $t = 60.0$, and (c) $t = 85.0$. The simulation shown was performed in a box of dimensions 50×50 using 15 random initial modes.

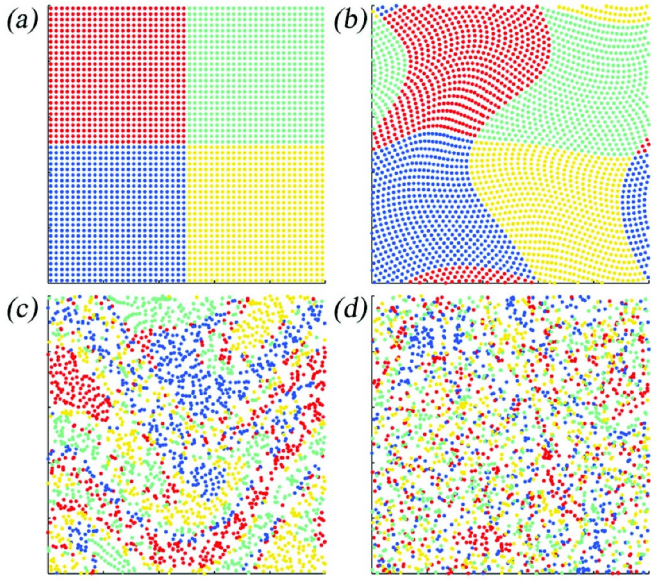

FIG. 4 (color online). Fluid mixing in the simulation of Fig. 3. The figure shows the distribution of fluid particles in the suspension at (a) $t = 0$, (b) $t = 30$, (c) $t = 60$, and (d) $t = 90$.

parameter. The concentration field also develops strong fluctuations at long wavelengths. The formation of these density fluctuations, which is not predicted by the linear stability analysis, may be shown to be driven by the concentration-weighted director field, which is not divergence-free and results in the aggregation of particles by their swimming velocity in regions of $\nabla_{\mathbf{x}} \cdot (c\mathbf{n}) < 0$ [20]. The dense regions are typically in the form of bands [Fig. 3(b)], which become unstable and fold onto themselves under the fluid disturbance flow [Fig. 3(c)]. After folding, the bands break up and reorganize in the transverse direction. These dynamics repeat quasiperiodically, and may be analogous to the ''jetting'' previously reported in experiments; cf. Fig. 4 of Ref. [7]. The magnitude of the density fluctuations in the simulations is found to be controlled by diffusion, which stabilizes the density gradients at long times.

We conclude by discussing the effect of these dynamics on fluid mixing. Figure 4 shows the evolution of fluid particle configurations over the course of a simulation. At short times, little mixing occurs as the fluid disturbance flow is quite weak. However, strong mixing starts to take place as the instability appears and the disturbance flow becomes stronger. The formation and break-up of the concentration bands results in stretching and folding of fluid elements, and at $t = 90$ (corresponding to approximately four stretch-fold cycles), efficient mixing has been achieved. Fluid mixing from fluid-body interaction has been reported in simulations [13,14] and experiments [5,22]: our simulations cast light on one origin for mixing, which is related to the constant break-up and merging of concentrated regions as a consequence of the active stress instability. It is worth noting that the experiments showing large-scale mixing were done using *B. Subtilis*, which is a pusher [7,8]. An apparent prediction of our theory is that such mixing flows would not be observed for suspensions of pullers, such as the microorganism *Chlamydomonas*.

The authors thank R. Goldstein and C. Hohenegger for useful conversations, and gratefully acknowledge the hospitality and support of the Aspen Center for Physics, where part of this work was performed. This work is supported by NSF Grant No. DMS-0412203 and DOE Grant No. DE-FG02-88ER25053.

*Present address: Department of Mechanical Science and Engineering, University of Illinois at Urbana-Champaign.

[1] T. J. Pedley and J. O. Kessler, Annu. Rev. Fluid Mech. **24**, 313 (1992).
[2] W. F. Paxton *et al.*, J. Am. Chem. Soc. **126**, 13424 (2004).
[3] R. Dreyfus *et al.*, Nature (London) **437**, 862 (2005).
[4] J. R. Howse *et al.*, Phys. Rev. Lett. **99**, 048102 (2007).
[5] M. J. Kim and K. S. Breuer, Phys. Fluids **16**, L78 (2004).
[6] X.-L. Wu and A. Libchaber, Phys. Rev. Lett. **84**, 3017 (2000).
[7] C. Dombrowski *et al.*, Phys. Rev. Lett. **93**, 098103 (2004).
[8] I. Tuval *et al.*, Proc. Natl. Acad. Sci. U.S.A. **102**, 2277 (2005).
[9] N. H. Mendelson *et al.*, J. Bacteriol. **181**, 600 (1999).
[10] G. V. Soni *et al.*, Biophys. J. **84**, 2634 (2003).
[11] A. Sokolov *et al.*, Phys. Rev. Lett. **98**, 158102 (2007).
[12] I. S. Aranson *et al.*, Phys. Rev. E **75**, 040901 (2007).
[13] J. P. Hernandez-Ortiz, C. G. Stoltz, and M. D. Graham, Phys. Rev. Lett. **95**, 204501 (2005).
[14] D. Saintillan and M. J. Shelley, Phys. Rev. Lett. **99**, 058102 (2007).
[15] T. Ishikawa and T. J. Pedley, J. Fluid Mech. **588**, 437 (2007).
[16] M. Doi and S. F. Edwards, *The Theory of Polymer Dynamics* (Oxford University Press, Oxford, 1986).
[17] R. A. Simha and S. Ramaswamy, Phys. Rev. Lett. **89**, 058101 (2002).
[18] G. B. Jeffery, Proc. R. Soc. A **102**, 161 (1922).
[19] G. K. Batchelor, J. Fluid Mech. **46**, 813 (1971).
[20] D. Saintillan and M. J. Shelley (to be published).
[21] In unpublished work, this extra branch has also been found by T. J. Pedley (private communication).
[22] M. B. Short *et al.*, Proc. Natl. Acad. Sci. U.S.A. **103**, 8315 (2006).